



Short communication

## Facile one-step fabrication of $\text{Li}_4\text{Ti}_5\text{O}_{12}$ coatings by suspension plasma spraying

Sribalaji Mathiyalagan<sup>a</sup>, Stefan Björklund<sup>a</sup>, Sandra Johansson Storm<sup>a</sup>, Girish Salian<sup>b</sup>, Ronan Le Ruyet<sup>b</sup>, Reza Younesi<sup>b</sup>, Shrikant Joshi<sup>a,\*</sup>

<sup>a</sup> University West, Department of Engineering Science, SE 461 86, Trollhättan, Sweden

<sup>b</sup> Department of Chemistry-Ångström Laboratory, Uppsala University, SE 75121, Uppsala, Sweden



## ARTICLE INFO

## Keywords:

LTO  
Fabrication  
Plasma spraying  
Suspension  
One-step

## ABSTRACT

Spinel  $\text{Li}_4\text{Ti}_5\text{O}_{12}$  (LTO) is a promising anode material for solid state thin film batteries (SSTB) due to its almost-zero volume change and promising Li-ion mobility. However, preparing LTO anodes for SSTB demands tedious vacuum-based processing steps that are not cost effective. In this context, the present study embarks on evaluating the versatile suspension plasma spraying (SPS) approach to fabricate LTO coatings without using any binder. The microstructure and stoichiometry of the fabricated LTO coatings developed through the SPS route reveals retention of  $\sim 76$  wt.% of the spinel LTO from the starting feedstock, with minor amounts of rutile and anatase  $\text{TiO}_2$ . The SPS experiments yielded varying thickness build up rates of the LTO coatings depending on the processing parameters adopted. The electrochemical data of the produced LTO based electrode tested in a half-cell through galvanostatic cycling show reversible lithiation and delithiation at expected potential, thereby validating the promise of the SPS technique for potential fabrication of SSTB components once fully optimized.

### 1. Introduction

Compared with rechargeable lithium-ion batteries using a liquid organic electrolyte, solid-state thin film batteries (SSTBs) are acknowledged to hold significant promise for improving safety of batteries [1]. The preparation methods for SSTB electrodes and electrolytes that have been investigated in the past have included Radio Frequency Magnetron Sputtering Deposition (RFMSD) [2], Pulsed Laser Deposition (PLD) [3], Electron Beam Evaporation (EBE) [4], Chemical Vapor Deposition (CVD) [5], Molecular Beam Epitaxy (MBE) [6]. However, most of the above coating techniques are vacuum-based, inappropriate for large-scale deposition and characterized by slow deposition rates as well as high cost. The above techniques have also been observed to yield mostly amorphous coatings, and crystallization of the as-deposited coatings is subsequently accomplished through an additional post-processing heat treatment step. However, the post-processing heat treatment is also known to result in undesired formation of secondary phases.

Notwithstanding the above, other innovative coating approaches that can potentially overcome the above shortcomings have not yet been assessed as potential pathways to fabricate SSTB components. Among

these are the liquid feedstock based thermal spray processes, specifically the suspension plasma spraying (SPS) technique. SPS, like other thermal spray techniques, presents certain key advantages over traditional vacuum-based routes as it enables rapid large area deposition of dense, uniform coatings with refined microstructure and high crystallinity [7, 8]. The thermal spray techniques allow deposition of a vast assortment of coatings (metallic or ceramic), with tailored microstructures (dense, porous and columnar) and function-dependent architectures (layered or composite) using suitable feedstock. The SPS, in particular, obviates challenges associated with feeding of fine powders (0.1–5  $\mu\text{m}$ ) and thereby facilitates deposition of uniform thin coatings with refined microstructures. Embracing such new coating techniques potentially presents a great opportunity to create a unique pathway to realize large-scale production of SSTB components.

This paper seeks to produce a binder-less lithium titanate ( $\text{Li}_4\text{Ti}_5\text{O}_{12}$ , hereafter known as LTO) anode using SPS technique as a first step towards demonstrating the capability of this facile approach to fabricate SSTB components. The choice of LTO as the coating material stems from its unique properties, including relatively high operating voltage as anode material ( $\sim 1.55$  V), decreasing the possibility of solid electrolyte interphase (SEI) formation, almost zero volume change ( $< 0.2\%$ ) and

\* Corresponding author.

E-mail address: [shrikant.joshi@hv.se](mailto:shrikant.joshi@hv.se) (S. Joshi).

<https://doi.org/10.1016/j.matresbull.2024.113111>

Received 1 April 2024; Received in revised form 12 September 2024; Accepted 25 September 2024

Available online 27 September 2024

0025-5408/© 2024 The Author(s). Published by Elsevier Ltd. This is an open access article under the CC BY license (<http://creativecommons.org/licenses/by/4.0/>).

promising Li-ion mobility [9-11]. This work, pursued as a proof-of-concept study, showcases the possibility of preparing a LTO suspension using a commercially available fine powder, identifying suitable process conditions to spray the suspension, and subsequently investigating the corresponding microstructural characteristics and phase constitution of the deposited LTO coatings. The electrochemical characterization of the LTO coatings provides preliminary insight into their performance as electrodes to highlight the promise of the SPS technique for further SSTB development.

## 2. Experimental methods

A stable LTO suspension with 20 wt.% solid load in deionized water was prepared using a commercially available LTO powder with particles size 1.5 - 3  $\mu\text{m}$  (NEI Corporation, USA). Since the initially prepared suspension was found to have very limited stability, three different additives, namely DISPERBYK-199 (BYK-Chemie GmbH, Germany), 1-Methyl-2-pyrrolidinone (NMP) (Sigma-Aldrich, Sweden), polyvinylpyrrolidone (PVP) (Sigma-Aldrich, Sweden) were tried. Among the above, 1 wt.% NMP addition to the suspension was found to yield optimum stability to enable spraying. The suspension was sprayed using an Axial III plasma gun (Northwest Mettech Corp., Canada) on 2 mm thick, 25 mm diameter aluminum (Al) substrates. The spray parameters used in this study are specified in Table 1. As depicted in the table, a total of four different LTO coatings were sprayed to study the effect of key spray process parameters (namely, nozzle type, enthalpy, feed rate and stand-off-distance) on the microstructure, stoichiometry, and electrochemical activity of the sprayed coatings.

The cross section of each deposited coating was observed after careful sample preparation. The specimens were first cold-mounted in a phenolic resin and the mounted sample slow precision cut (IsoMet 5000, Buehler, USA) with a diamond blade prior to remounting using standard metallographic procedure. The coating cross-sections were studied in a table-top scanning electron microscope (Hitachi TM3000, Hitachi, Japan) in backscattered electron (BSE) mode, while the phase composition of the starting powder and all the four coatings were analyzed by a Bruker D8 diffractometer (Bruker, Germany). The acquisition of the diffraction patterns was done using Cu  $K\alpha_1$ - $K\alpha_2$  radiation in a  $\theta$  -  $\theta$  configuration within a  $2\theta$  range of 10–70°. Rietveld refinement of the diffraction data obtained from the XRD scan was done using TOPAS software (Bruker, Germany). For testing electrochemical activity, LTO electrodes were cycled in pouch cells assembled in an argon filled glovebox (< 1 ppm of  $\text{O}_2$  and < 1 ppm of  $\text{H}_2\text{O}$ ). LP40, i.e. 1 M of  $\text{LiPF}_6$  in EC:DEC (1:1 vol ratio) electrolyte added to a glass fiber separator was used. The cells were cycled at C/20 considering an active mass of 59.9 mg and the theoretical capacity of LTO (i.e. 175 mAh/g) 2.5 to 0.5 V vs.  $\text{Li}^+/\text{Li}$  using a LAND potentiostat.

## 3. Results and discussion

Fig. 1(a-d) show the cross-sectional micrographs of LTO coatings processed under different spray conditions indicated in Table 1. The micrographs reveal that the thickness of the LTO coatings deposited for an identical number of spray passes, which is a measure of the deposition efficiency, varies with spray variables employed. As has been widely reported, the deposition characteristics in plasma sprayed

coatings are significantly influenced by processing conditions, with there being a complex interplay between the primary variables varied in this study. In plasma spraying, complete melting of the powder particles is usually a prerequisite for good deposition efficiency and high particle velocity is desirable for good adhesion of the coatings which are mechanically anchored to the substrate. In this case, a higher enthalpy directly translates into more thermal energy in the plasma plume to promote gas-particle heat transfer. On the other hand, the nozzle diameter has a twin effect - all else being identical, a smaller nozzle diameter leads to a higher gas velocity being available for particle acceleration, but this also reduces the residence time of the particles in the plasma plume. The spray distance, too, is important since it influences the evolution of particle temperature and velocity prior to impact with the substrate. LTO is reported to have a melting point of just above 1500 °C. The available thermal energy and residence time need to be adequate for complete melting but should not lead to dissociation/phase change in the LTO in flight. It is interesting to note that use of the smaller 5/16 nozzle with high enthalpy of 11 KJ and a slightly higher standoff distance yielded the thickest coating in the present study.

Further, microstructural features observed in the coatings appear to depict a multi-phase constitution as suggested by the light and dark gray areas present in the cross-section micrographs, which are more clearly evident in coatings R3, R4 and R5. A high magnification micrograph of R5 coating depicted in Fig. 1(e) shows the light gray regions (marked as point 1) to be denser compared to the relatively more porous dark gray regions (marked as point 2). EDS analysis on the two regions showed the light gray regions are richer in Ti than the dark gray region. It is to be noted that it is impossible to detect Li using EDS. However, the difference in Ti atomic percentage between points 1 and 2 is clearly indicative of some degree of phase transformation during the spraying process. Therefore, in order to understand the changes in phase constitution that occur during spraying, XRD analysis was conducted on all the four coatings along with the commercial LTO powder used for deposition.

The XRD patterns presented in Fig. 2a show that the sprayed LTO coatings have undergone partial amorphization during spraying, as reflected in the reduced intensity of the peaks with a corresponding increase in the respective peak's full width at half maximum (FWHM). This is in comparison to the XRD pattern of the as-received powder used to prepare the suspension feedstock. Ramsdellite lithium titanate ( $\text{Li}_2\text{Ti}_3\text{O}_7$ ) is also detected to have formed as one of the crystalline phases in the deposited coatings. This could be attributed to the partial delithiation of the LTO that could have occurred during spraying. Delithiation of LTO is known to occur at high temperature in the presence of oxygen. Some low intensity aluminum peaks are also noted in the XRD patterns of R2, R3, and R4. The aluminum signal, which can come from the underlying substrate, was absent in the R5 coating due to the higher thickness of the overlay LTO coating.

Since the coating sample R5 represented the most promising spray conditions among those utilized in the present study, Rietveld refinement analysis was performed on its diffractogram to analyze the different phases present (Fig. 2b). This refinement shows that LTO spinel structure remains its main constituent phase at 76.23 wt.% while the partially delithiated ramsdellite phase ( $\text{Li}_2\text{Ti}_3\text{O}_7$ ) contributes 18.99 wt.%. The fully delithiated rutile  $\text{TiO}_2$  was found to be 4.62 wt.% and anatase  $\text{TiO}_2$  was just 0.16 wt.%. It is pertinent to emphasize here that this paper is an important first step towards demonstrating the capability of the facile SPS approach to fabricate SSTB components, beginning with the LTO layer deposition discussed herein. While the immediate intent of this study was to demonstrate that this novel approach bears promise, the SPS deposition process will need to be meticulously optimized since it is influenced by numerous factors such as the LTO particle size, extent of solid loading, suspension characteristics and a host of plasma spray parameters (nozzle diameter, plasma enthalpy, stand-off distance etc.).

Galvanostatic cycling of the R5 coating in Fig. 3 shows the expected potential reaction for the lithiation/delithiation of LTO at about 1.56 V

**Table 1**

SPS process parameters used for depositing LTO coatings.

Sample code	Nozzle dia (inches)	Enthalpy (kJ)	Feed rate (ml/min)	Stand-off distance (mm)
R2	3/8	8	40	60
R3	3/8	11	40	60
R4	5/16	7.5	42	60
R5	5/16	11	42	70

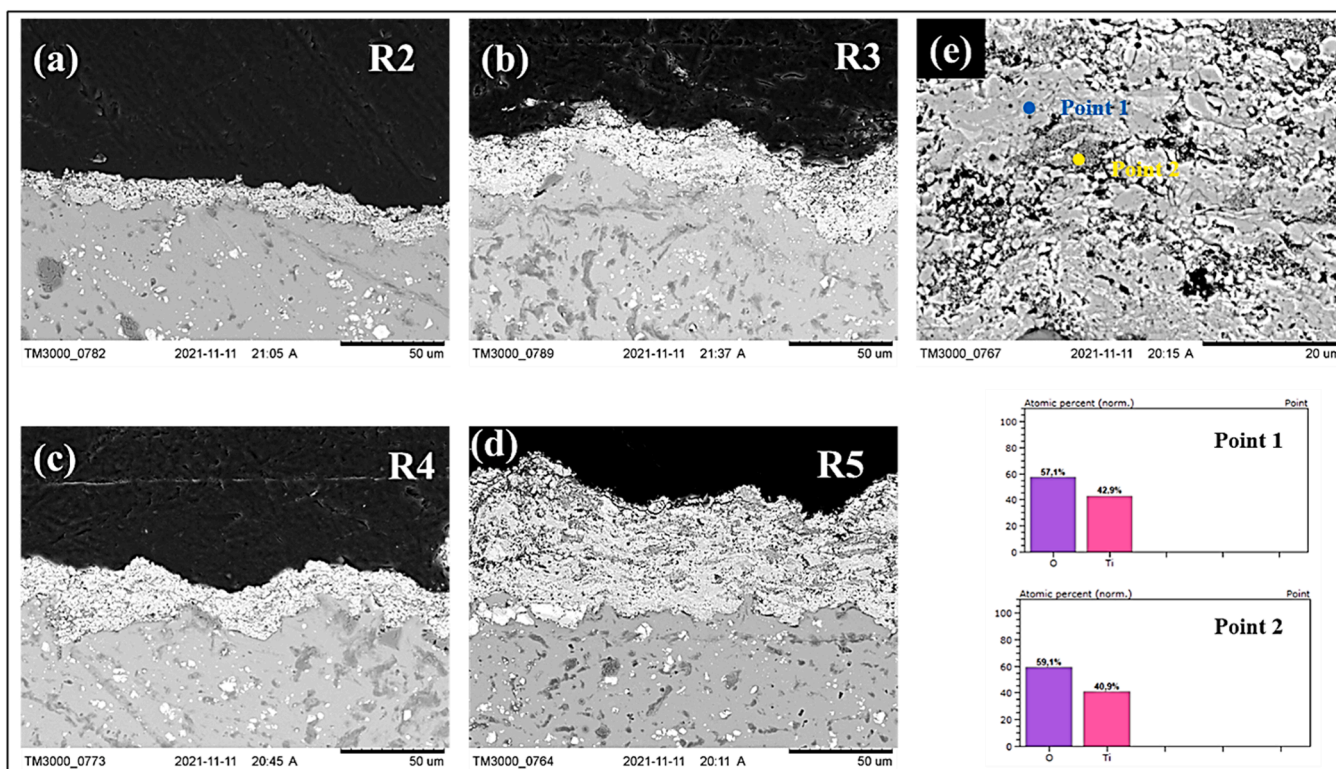


Fig. 1. (a-d) Cross-section micrographs of the four LTO coatings (i.e. R2, R3, R4 and R5), (e) high magnification image of R5 coating and the EDS spectra corresponding to points 1 and 2 marked in (e).

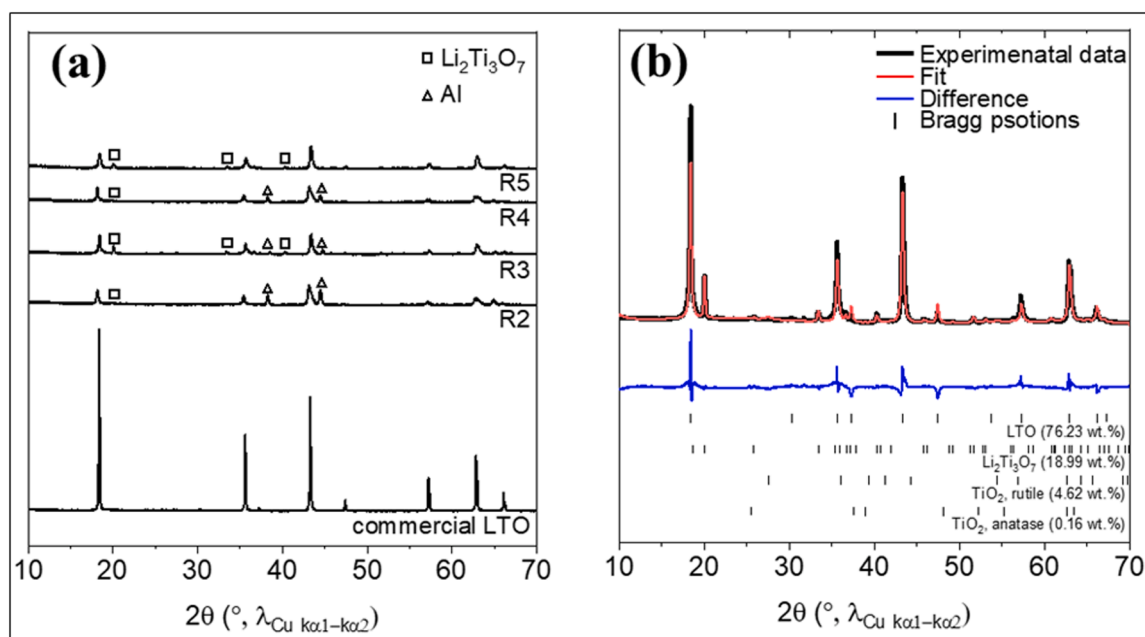
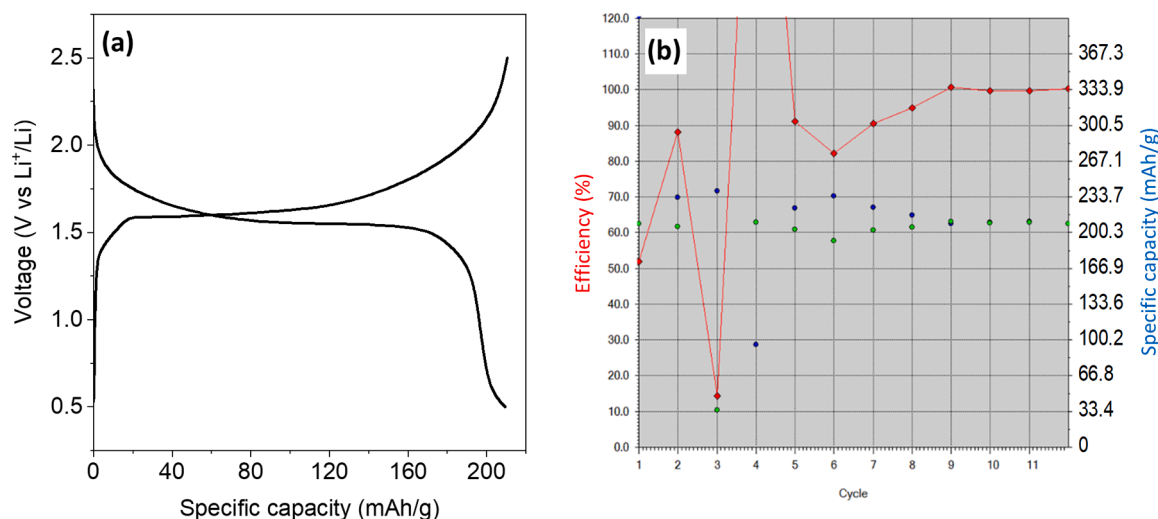


Fig. 2. (a) XRD patterns obtained for commercial LTO power and the four LTO coatings (R2, R3, R4 and R5) obtained with different spray parameters, (b) Rietveld refinement of the diffractogram of R5 coating.

vs.  $\text{Li}^+/\text{Li}$  [12–14]. The mass of LTO in this sample was estimated to be 59.9 mg by assuming that the substrate was a perfect disk of aluminum with a diameter of 25 mm and a thickness of 2 mm and by subtracting its assumed mass (2650.7 mg) from that of the mass of the coated electrode (2710.6 mg). These assumptions lead to an observed capacity of 211 mAh/g which exceeds the theoretical value of 175 mAh/g [13]. The higher numerical value of the observed capacity could be due to an

underestimation of the coated LTO mass but strongly suggests that the associated reaction is mainly the lithiation and delithiation of LTO. Additionally, it also raises prospects of exploring the SPS route further to deposit electrolyte and cathode layers to construct the entire SSTB cell.



**Fig. 3.** Galvanostatic cycling of the sample R5 in a half-cell using Li as counter electrode and 1 M LiPF<sub>6</sub> in EC:DEC as electrolyte showing (a) the voltage versus specific capacity curve in charge and discharge of cycle 10 and (b) the values of specific in charge (blue points) and discharge (green points), as well as the coulombic efficiency (red points) as a function of the cycle numbers.

#### 4. Conclusion

In summary, we have demonstrated single step processing of LTO coatings by adopting a facile suspension plasma spraying route. Nozzle configuration, plasma plume enthalpy and spray distance were found to influence LTO coating deposition. The microstructure of the LTO coatings revealed a multi-phase structure indicative of phase change during spraying. However, investigation of the LTO coating representing the most promising spray conditions among those studied, revealed the LTO spinel structure to remain the prominent constituent phase with the partially delithiated phase Li<sub>2</sub>Ti<sub>3</sub>O<sub>7</sub> contributing a majority of the rest and the fully delithiated TiO<sub>2</sub> phase presence being negligible. Galvanostatic cycling of the coating showed the expected potential reaction for the lithiation/delithiation of LTO at about 1.56 V vs. Li<sup>+</sup>/Li with a specific capacity indicating the full lithiation and delithiation of LTO. While the quality of the LTO deposited by SPS can clearly be further improved by process optimization to reduce its decomposition during spray processing, the study established that it is a possible route to fabricate LTO anodes on Aluminum substrates and perhaps for further exploration to sequentially deposit the anode-electrolyte-cathode layers to construct SSTBs in half-cell and full-cell configurations.

#### Declaration of Generative AI in scientific writing

The authors declare that no AI tools were used for any part of this manuscript.

#### Submission declaration

The work described has not been published previously (except in the form of an academic thesis), is not under consideration for publication elsewhere, and its publication is approved by all authors and tacitly or explicitly by the responsible authorities where the work was carried out; if accepted, it will not be published elsewhere in the same form, in English or in any other language, including electronically without the written consent of the copyright-holder.

#### CRediT authorship contribution statement

**Sribalaji Mathiyalagan:** Writing – original draft, Methodology, Investigation. **Stefan Björklund:** Writing – review & editing, Investigation. **Sandra Johansson Storm:** Investigation. **Girish Salian:**

Investigation. **Ronan Le Ruyet:** Writing – original draft, Methodology, Investigation. **Reza Younesi:** Writing – review & editing, Project administration, Methodology, Funding acquisition. **Shrikant Joshi:** Writing – review & editing, Project administration, Methodology, Funding acquisition, Conceptualization.

#### Declaration of competing interest

The authors declare the following financial interests/personal relationships which may be considered as potential competing interests: Shrikant Joshi reports financial support was provided by Swedish Energy Agency. If there are other authors, they declare that they have no known competing financial interests or personal relationships that could have appeared to influence the work reported in this paper.

#### Data availability

The data that has been used is confidential.

#### Acknowledgement

The financial support from Energimyndigheten, Sweden for the financial support under which this work was carried out (Project Novel-CABs, P46393-1) is gratefully acknowledged. The authors also thank Mr. Magnus Sandberg, University West, for his assistance in spraying the coatings.

#### References

- [1] Y. Chen, K.H. Wen, T.H. Chen, et al., Recent progress in all-solid-state lithium batteries: The emerging strategies for advanced electrolytes and their interfaces, *Energy Storage Mater.* 31 (2020) 401–433.
- [2] S. Pat, S. Özen, H.H. Yudar, et al., The transparent all-solidstate rechargeable micro-battery manufacturing by RF magnetron sputtering, *J. Alloys. Compd.* 713 (2017) 64–68.
- [3] Y. Matsuda, N. Kuwata, J. Kawamura, Thin-film lithium batteries with 0.3–30 μm thick LiCoO<sub>2</sub> films fabricated by high-rate pulsed laser deposition, *Solid. State Ion.* 320 (2018) 38–44.
- [4] M. Choi, S.H. Lee, Y.I. Jung, et al., The high capacity and cycle stability of NiFe<sub>2</sub>O<sub>4</sub> thin film prepared by E-beam evaporation method for lithium ion batteries, *J. Alloys. Compd.* 729 (2017) 802–808.
- [5] H.B. Shi, H. Zhang, X.X. Li, et al., In situ fabrication of dual coating structured SiO<sub>2</sub>/1D-C/a-C composite as high-performance lithium ion battery anode by fluidized bed chemical vapor deposition, *Carbon. N. Y.* 168 (2020) 113–124.

- [6] T. Chen, F.B. Meng, Z.W. Zhang, et al., Stabilizing lithium metal anode by molecular beam epitaxy grown uniform and ultrathin bismuth film, *Nano Energy* 76 (2020) 105068.
- [7] R. Haese, L. Pawlowski, M. Bigan, R. Jaworski, M. Martel, Phase evolution of hydroxapatite coatings suspension plasma sprayed using variable parameters in simulated body fluid, *Surf. Coat. Tech.* 204 (8) (2010) 1236–1246.
- [8] L. Pawlowski, Suspension and Solution thermal spray coatings, *Surf. Coat. Tech.* 203 (19) (2009) 2807–2829.
- [9] Y. Yang, B. Qiao, X. Yang, L. Fang, C. Pan, W. Song, H. Hou, X. Ji, Lithium titanate tailored by cathodically induced graphene for an ultrafast lithium ion battery, *Adv. Funct. Mater.* 24 (2014) 4349–4356.
- [10] C.P. Han, Y.B. He, M. Liu, B.H. Li, Q.H. Yang, C.P. Wong, F.Y. Kang, A review of gassing behavior in Li<sub>4</sub>Ti<sub>5</sub>O<sub>12</sub> based lithium ion batteries, *J. Mater. Chem.* 5 (2017) 6368–6381.
- [11] T. Nordh, R. Younesi, D. Brandell, K. Edström, Depth profiling the solid electrolyte interphase on Lithium Titanate (Li<sub>4</sub>Ti<sub>5</sub>O<sub>12</sub>) using synchrotron-based photoelectron spectroscopy, *J. Power Sources* 294 (2015) 173–179.
- [12] W.J.H. Borghols, M. Wagemaker, U. Lafont, E.M. Kelder, F.M. Mulder, *J. Am. Chem. Soc.* 131 (2009) 17786–17792.
- [13] M. Wagemaker, E.R.H. van Eck, A.P.M. Kentgens, F.M. Mulder, *J. Phys. Chem. B* 113 (2009) 224–230.
- [14] S. Sarciaux, A.L.G. La Salle, D. Guyomard, Y. Piffard, *Mol. Cryst. Liq. Cryst. Sci. Technol. Sect. A. Mol. Cryst. Liq. Cryst.* 311 (1998) 63–68.